Journal of Materials Chemistry A

ROYAL SOCIETY OF CHEMISTRY

PAPER

View Article Online
View Journal | View Issue

Open Access Article. Published on 26 Waysu 2022. Downloaded on 26/08/2024 11:52:58 AM.
This article is licensed under a Creative Commons Attribution-NonCommercial 3.0 Unported Licence.

Check for updates

Cite this: J. Mater. Chem. A, 2022, 10, 25085

# Biobased catalyst-free covalent adaptable networks based on $CF_3$-activated synergistic aza-Michael exchange and transesterification†

Dimitri Berne, Baptiste Quienne, Sylvain Caillol, Eric Leclerc * and Vincent Ladmiral *

Received 26th June 2022
Accepted 26th September 2022

DOI: 10.1039/d2ta05067f

rsc.li/materials-a

Recently, fluorine neighboring group activation emerged as a new way of promoting acid–epoxy reaction and transesterification in vitrimer materials. Pursuing this idea, the effect of a $CF_3$ group on aza-Michael addition and aza-Michael exchange was examined and confirmed on model molecules. Following these positive results, a CAN incorporating aza-Michael bonds and $CF_3$-activated ester functions was synthesized and compared to analogous materials deprived of any $CF_3$ groups on the one hand, or of any hydroxyl groups on the other hand. The study of the mechanical properties of these materials highlighted the synergistic effect of the two exchange reactions and the accelerating effect of the fluorinated group. The fluorinated and hydroxylated material was shown to be reprocessable at 100 °C in 1 h under 3 tons whereas the fluorinated only and the hydroxylated only materials were respectively reprocessed at 120 °C and 150 °C. These catalyst-free CANs were synthesized from natural resources further enhancing the sustainability of these materials. This study demonstrates the potential of biobased CANs featuring fluorinated esters as low environmental impact and easily reprocessable materials.

## Introduction

Covalent Adaptable Networks (CANs) have emerged in the last two decades as a new polymer family, bridging the gap between the two historical groups of polymers: thermoplastics and thermosets. CANs refer to polymer networks possessing reversible covalent bonds, hence coupling the reshaping capability of thermoplastics with the thermal and chemical resistance of thermosets. The development of CANs is going in the same direction as the current environmental trend of reducing waste and improving the sustainability of materials. Indeed, cross-linked polymers, whose recycling is particularly complex,[1] can gain the possibility of being reused instead of only being incinerated if they are converted into CANs. Their recycling through the dynamic character of CANs can then be triggered by different stimuli such as heat,[2] pH[3] or light.[4]

The area of CANs is in constant development and multiple exchangeable functions have emerged and have been reviewed by several research team.[5–8] They have been generally classified according to their mechanism: dissociative or associative.[9] Theoretically, in opposition to dissociative CANs, only vitrimers (associative CANs) maintain a constant crosslink density with temperature and can therefore demonstrate an Arrhenius behaviour.[10–15] However, numerous dissociative CANs have recently demonstrated Arrhenius behavior in specific ranges of temperature.[16–21] Moreover, Dichtel and Elling have been wondering whether the use of associative exchange mechanism alone in cross-link polymer networks was desirable to meet current processing challenges.[22] Indeed, as dissociative and associative CANs demonstrated to behave similarly in temperature range usually used for reprocessing, the postulated superiority of vitrimers on dissociative CANs should be reconsidered. Especially since the use of dissociative chemistries could enable to respond to some current CAN challenges (synthesis of high activation energy CANs, adaptation of current thermoplastics reprocessing techniques to CANs, broad CANs application range *via* the development of new exchange reactions,…).[7]

Many of the dynamic chemistries mentioned above require catalysts to be activated under thermal stimulus.[23,24] However, the use of external catalysts is limiting the panel of applications of CANs. For instance, organic salts[25,26] and strong bases,[27] used as catalysts in epoxy vitrimers, are usually toxic and corrosive, and may leach out from the materials or undergo ageing.[28] Therefore, the concepts of neighbouring group participation (NGP) or internal catalysis inspired from development in organic synthesis have been implemented in CANs.[29,30] Several modes of activation have been reported in the literature such as H-bonding,[31–33] formation of cyclic intermediate[34,35] or tertiary amine catalyst.[36,37] Recently, the introduction of fluorinated

ICGM, Université Montpellier, CNRS, ENSCM, Montpellier, France. E-mail: vincent.ladmiral@enscm.fr; eric.leclerc@enscm.fr

† Electronic supplementary information (ESI) available. See https://doi.org/10.1039/d2ta05067f

Open Access Article. Published on 26 Waysu 2022. Downloaded on 26/08/2024 11:52:58 AM.
This article is licensed under a Creative Commons Attribution-NonCommercial 3.0 Unported Licence.

groups near an ester function allowed to significantly increase the transesterification reaction rate *via* inductive effects.[38–40]

Based on these precedents, we wished to explore the possibility of designing a CAN that could relax according to two possible exchange reactions, both sufficiently accelerated by a single activating group to avoid the presence of any external catalyst. This dual mechanism could lead to a network with strong dynamical properties and, coupled to a biosourcing of the monomer and the absence of any additive, it would reinforce the durability and recyclability of such material. We already reported that catalyst-free transesterification vitrimers could be prepared and exhibit vitrimer properties thanks to the presence of vicinal fluorinated groups that accelerate the exchange reaction.[38] We wish to present herein a material that associates this transesterification to a much less studied reaction, namely the aza-Michael exchange.[41,42] In this synergistic system, both reactions are activated by the same $CF_3$ group positioned on the α-position to the ester. The effect of the $CF_3$ group was first highlighted on the aza-Michael addition and aza-Michael exchange reactions on model compounds. Then, a set of CANs constituted of β-amino esters was synthesized by aza-Michael polyaddition. Bio-based *bis*-hydroxylated amine and *bis*-trifluoromethylacrylate were used to synthesize a CAN coupling synergistic and fluorine accelerating effect with a high renewable carbon content. Its non-fluorinated analogue, as well as the one devoid of hydroxy groups were also prepared in order to assess the influence of each group on the mechanical behaviour of the materials. The thermal and stress relaxation behaviours of these materials were evaluated by mechanical and chemical analyses. Finally, these materials were reshaped three times under different conditions and the influence of the reprocessing conditions on the materials was studied. This study highlights how the incorporation of fluorine exchange activator, and synergistic exchange reactions in cross-linked networks, enables to easily synthesize and recycle sustainable materials.

## Materials & methods

### Materials

Butanediol diglycidyl ether (BDGE), 4,9-dioxadodecanediamine (BDA), 2-methyltetrahydrofurane (Me-THF) and *N*-benzylmethylamine (BMA) were purchased Sigma-Aldrich Merck (Darmstadt, Germany). Aqueous ammonia (25% $NH_3$) were purchased from VWR International S. A. S (Fontenay-sous-Bois, France). Pripol™ 2033 was kindly provided by Croda (East Cowick, United Kingdom). 2-(Trifluoromethyl)acrylic acid (MAF) (>98%), *tert*-butyl 2-(Trifluoromethyl)acrylate (MAF-TBE) and methyl 2-(trifluoromethyl)acrylate (MAF-Me) were purchased from SynQuest Labs (Alachua, FL, USA). All materials were used as received. The deuterated NMR solvents ($CDCl_3$ (99.5% isotopic purity), MeOD (99.5% isotopic purity) and DMF-$d_7$ (99.5% isotopic purity)) and were purchased from Eurisotop (Saint-Aubin, France).

### Characterizations

**Nuclear magnetic resonance.** Nuclear Magnetic Resonance ($^1$H, $^{13}$C, $^{19}$F-NMR) experiments were carried out in deuterated solvents using a Bruker Avance III 400 MHz NMR spectrometer at 25 °C.

**Titration of the amine equivalent weight of Priamine™1071 by $^1$H-NMR.** The Amine Equivalent Weight (AEW) is the amount of product needed for one equivalent of reactive amine function. It was determined by $^1$H-NMR using an internal standard (benzophenone). A known mass of product and benzophenone was poured into an NMR tube and 500 μL of $CDCl_3$ were added. The AEW was determined using eqn (1) by comparing the value of the integral of the signals assigned to the benzophenone protons (7.5–7.8 ppm) with the value of the integral of the signals arising from the CH protons in β position to the primary (3.72 ppm) and secondary (3.88 ppm) amine groups. The measurement of the AEW was performed in triplicate.

$$\mathrm{AEW} = \left(\frac{\int \mathrm{PhCOPh} \times \mathrm{H_{amineI}}}{\int \mathrm{amineI} \times \mathrm{H_{PhCOPh}}} + \frac{\int \mathrm{PhCOPh} \times \mathrm{H_{amineII}}}{2 \times \int \mathrm{amineII} \times \mathrm{H_{PhCOPh}}}\right) \times \frac{m_{\mathrm{amine}}}{m_{\mathrm{PhCOPh}}} \times M_{\mathrm{PhCOPh}} \quad (1)$$

$\int_{\mathrm{PhCOPh}}$: integral of the signal from benzophenone protons; $\int_{\mathrm{amineI}}$: integral of the signals from protons in α of the primary amine function; $\int_{\mathrm{amineII}}$: integral of the signals from protons in α position of the secondary amine function; $\mathrm{H_{amineI}}$: number of protons in α position of the primary amine function; $\mathrm{H_{amineII}}$: number of protons in α position of the secondary amine function $\mathrm{H_{PhCOPh}}$: number of benzophenone protons; $m_{\mathrm{amine}}$: mass of amine; $m_{\mathrm{PhCOPh}}$: mass of benzophenone; $M_{\mathrm{PhCOPh}}$: benzophenone molar mass.

**Fourier transform infrared spectroscopy.** Infrared (IR) spectra were recorded on a Nicolet 210 Fourier transform infrared (FTIR) spectrometer. The characteristic IR absorptions mentioned in the text are reported in cm$^{-1}$. Materials analyses were recorded using an ATR accessory.

**Thermogravimetric analyses.** Thermogravimetric analyses (TGA) were carried out using TG 209F1 apparatus (Netzch). Approximately 10 mg of sample were placed in an aluminum crucible and heated from room temperature to 580 °C at a heating rate of 20 °C min$^{-1}$ under nitrogen atmosphere (60 mL min$^{-1}$).

**Differential scanning calorimetry.** Differential Scanning Calorimetry (DSC) analyses were carried out using a NETZSCH DSC200F3 calorimeter, which was calibrated using indium, *n*-octadecane and *n*-octane standards. Nitrogen was used as purge gas. Approximately 10 mg of sample were placed in a perforated aluminum pan and the heat exchanges were recorded between −150 °C and 150 °C at 20 °C min$^{-1}$ to observe the glass transition temperature. The $T_g$ values were measured on the second heating ramp to erase the thermal history of the polymer. All the reported characteristic temperatures are average values of three measurements.

**Dynamic mechanical analyses.** Dynamic mechanical analyses (DMA) were carried out on Metravib DMA 25 with Dynatest 6.8 software. Samples were tested in the uniaxial tension mode at a frequency of 1 Hz with a fixed strain of 10$^{-5}$ m, while applying a temperature ramp at a rate of 3 °C min$^{-1}$ from

Open Access Article. Published on 26 Waysu 2022. Downloaded on 26/08/2024 11:52:58 AM. This article is licensed under a Creative Commons Attribution-NonCommercial 3.0 Unported Licence.

−100 °C to +150 °C. The alpha transition temperature ($T_\alpha$) was determined as the maximum of the loss modulus $E''$.

**Rheology experiments.** Rheology experiments were performed on a ThermoScientific Haake Mars 60 rheometer equipped with a lower electrical temperature module and an active upper heating system, with a textured 8 mm plane–plane geometry. For all rheology experiments, the applied stress was comprised in the linear viscoelastic region. A 1 N axial force was applied to ensure proper contact between the plates and the samples for all experiments. For stress-relaxation experiments, a 1% shear strain was applied on samples, and the rubbery modulus evolution with time was monitored at different isotherms. The obtained characteristic relaxation time ($\tau$) was used to calculate the activation energy. The reproducibility of the analysis has been verified for at least one temperature for each sample for the stress-relaxation measurements.

Creep recovery experiments were performed at 80 °C and 50 °C by applying 2 kPa shear stress for a duration of 1200 s followed by a recovery period of 1200 s.

**Swelling index.** Three samples from the same material, of around 20 mg each, were separately immersed in THF for 24 h. The swelling index (SI) was calculated using eqn (2), where $m_2$ is the mass of the swollen material and $m_1$ is the initial mass. Reported swelling index are average values of the three samples.

$$\mathrm{SI} = \frac{m_2 - m_1}{m_1} \times 100 \quad (2)$$

**Gel content.** Three samples from the same material, of around 20 mg each, were separately immersed in THF for 24 h. The samples were then dried in a ventilated oven at 70 °C for 24 h. The gel content (GC) was calculated using eqn (3), where $m_3$ is the mass of the dried material and $m_1$ is the initial mass. Reported gel content are average values of the three samples.

$$\mathrm{GC} = \frac{m_3}{m_1} \times 100 \quad (3)$$

## Synthesis

**Synthesis of BMA-MAF-TBE.** *N*-Benzylmethylamine (BMA) (0.93 g, 7.70 mmol, 1 equiv.) was dissolved in dichloromethane (3 mL) and *tert*-butyl 2-(trifluoromethyl)acrylate (MAF-TBE) (1.51 g, 7.70 mmol, 1 equiv.) was slowly added to the solution at room temperature and stirred for 10 min. The pure product was obtained as a transparent liquid without any purification step. Yield: 99%, 2.44 g.

$^1$H-NMR (400 MHz, $CDCl_3$): 1.52 s, O–C–($C\underline{H}_3$)$_3$, 2.23 (s, N–$CH_3$), 2.69–2.73 (dd, $^3J$ = 12.5 Hz $^2J$ = 4.0 Hz, N–C$\underline{H}_2$–CH), 3.12–3.18 (m, N–$CH_2$–C$\underline{H}$), 3.26–3.36 (m, N–C$\underline{H}_2$–CH) 3.49–3.64 (m, N–C$\underline{H}_2$–C), 7.25–7.35 (m, $\underline{H}$Ar) $^{13}$C-NMR (101 MHz, $CDCl_3$): 27.9 (O–C–($\underline{C}H_3$)$_3$), 41.9 (N–$\underline{C}H_3$), 50.3–51.0 (q, $^2J$ = 25.7 Hz, N–$CH_2$–$\underline{C}$H), 54.0 (q, $^3J$ = 2.6 Hz, N–$\underline{C}H_2$–CH), 62.3 (N–$\underline{C}H_2$–C), 82.5 (O–$\underline{C}$–($CH_3$)$_3$), 120.3–129.2 (q, $\underline{C}F_3$), 127.2 (CH–CH–$\underline{C}$H–CH–CH), 128.2 ($\underline{C}$Ar), 128.9 ($\underline{C}$H–CH–CH–CH–$\underline{C}$H), 138.5 ($\underline{C}$–$CH_2$–N), 166.0 (q, $^3J$ = 3.4 Hz, $\underline{C}$=O) $^{19}$F-NMR (377 MHz, $CDCl_3$): $\delta$/ppm = - 67.3 ($CF_3$).

**Synthesis of BMA-MAF-Me.** *N*-Benzylmethylamine (BMA) (0.93 g, 7.70 mmol, 1 equiv.) was dissolved in dichloromethane (3 mL) and methyl 2-(trifluoromethyl)acrylate (MAF-Me) (1.19 g, 7.70 mmol, 1 equiv.) was slowly added to the solution at room temperature and stirred for 10 min. The pure product was obtained as a transparent liquid without any purification step. Yield: 99%, 2.10 g.

$^1$H-NMR (400 MHz, $CDCl_3$): 2.26 (s, N–$CH_3$), 2.73–2.77 (dd, $^3J$ = 12.6 Hz $^2J$ = 4.2 Hz, N–C$\underline{H}_2$–CH), 3.17–3.22 (m, N–$CH_2$–C$\underline{H}$), 3.42–3.51 (m, N–C$\underline{H}_2$–CH) 3.49–3.68 (m, N–C$\underline{H}_2$–C), 3.82 (s, O–C$\underline{H}_3$), 7.28–7.38 (m, $\underline{H}$Ar).

$^{13}$C-NMR (101 MHz, $CDCl_3$): 42.0 (N–$\underline{C}H_3$), 49.3–50.0 (q, $^2J$ = 26.3 Hz, N–$CH_2$–$\underline{C}$H), 52.7 (O–$\underline{C}H_3$), 53.7 (q, $^3J$ = 2.7 Hz, N–$\underline{C}H_2$–CH), 62.3 (N–$\underline{C}H_2$–C), 82.5 (O–$\underline{C}$–($CH_3$)), 120.0–128.2 (q, $^1J$ = 280.2 Hz, $\underline{C}F_3$), 127.3 (CH–CH–CH–CH–CH), 128.3 ($\underline{C}$Ar), 128.9 ($\underline{C}$H–CH–CH–CH–$\underline{C}$H), 138.3 ($\underline{C}$–$CH_2$–N), 167.4 (q, $^3J$ = 3.4 Hz, $\underline{C}$=O).

$^{19}$F-NMR (377 MHz, $CDCl_3$): $\delta$/ppm = −67.10–67.12 ($CF_3$).

**Synthesis of BMA-A-TBE.** *N*-Benzylmethylamine (BMA) (1.21 10 mmol, 1 equiv.) was mixed with *tert*-butyl acrylate (A-TBE) (1.54 g, 12 mmol, 1 equiv.) at 70 °C for 24 h. The crude product was dissolved into ethyl acetate (30 mL), washed three times with water (10 mL) and once with brine (10 mL). The organic layer was then dried over $MgSO_4$, dried under vacuum and the pure product was obtained as a transparent liquid. Yield: 85%, 2.12 g.

$^1$H-NMR (400 MHz, $CDCl_3$): $\delta$/ppm = 1.48 s, O–C–($C\underline{H}_3$)$_3$, 2.22 (s, N–$CH_3$), 2.45–2.49 (t, $^3J$ = 7.4 Hz, N–$CH_2$–C$\underline{H}_2$), 2.72-2.77 (t, $^3J$ = 7.4 Hz, N–C$\underline{H}_2$–$CH_2$), 3.53 (s, N–C$\underline{H}_2$–C), 7.26–7.34 (m, C$\underline{H}$–C$\underline{H}$–C$\underline{H}$–C$\underline{H}$–C$\underline{H}$).

$^{13}$C-NMR (101 MHz, $CDCl_3$): $\delta$/ppm = 28.1 (O–C–($\underline{C}H_3$)$_3$), 34.1 (N–$CH_2$–$\underline{C}H_2$), 41.8 (N–$\underline{C}H_3$), 53.1 (N–$\underline{C}H_2$–$CH_2$), 62.1 (N–$\underline{C}H_2$–C), 80.3 (O–$\underline{C}$–($CH_3$)$_3$), 127.0 (CH–CH–$\underline{C}$H–CH–CH), 128.2 (CH–$\underline{C}$H–CH–$\underline{C}$H–CH), 129.0 ($\underline{C}$H–CH–CH–CH–$\underline{C}$H), 139.1 ($\underline{C}$–$CH_2$–N), 172.0 ($\underline{C}$=O).

**Synthesis of butanediol-di-β-hydroxyamine (BD-β-HA).** BDGE (15 g, 0.15 mol, 1 equiv.) was dissolved in 232 mL of a 25% $NH_3$ aqueous solution (1.5 mol, 10 equiv.) and 232 mL of Me-THF in a 600 mL sealed reactor. The reaction was carried out at 100 °C for 4 h. The ammonia solution was then evaporated with a rotatory evaporator and then freeze-dried to remove water traces. The pure product was obtained as a brown viscous liquid. Yield: 99%, 20 g.

$^1$H-NMR (400 MHz, $CD_3OD$): $\delta$/ppm = 1.67 (m, $CH_2$–C$\underline{H}_2$–$CH_2$), 2.55–2.83 (m, C$\underline{H}_2$–NH–$CH_2$ and C$\underline{H}_2$–$NH_2$), 3.45 (d, CH–C$\underline{H}_2$–O), 3.52 (t, $CH_2$–C$\underline{H}_2$–O), 3.72 (m, C$\underline{H}$–OH), 3.88 (m, NH–$CH_2$–C$\underline{H}$–OH).

$^{13}$C-NMR (101 MHz, $CD_3OD$): $\delta$/ppm = 26.1 ($CH_2$–$\underline{C}H_2$–$CH_2$), 44.4 ($\underline{C}H_2$–$NH_2$), 52.4 ($\underline{C}H_2$–NH–$\underline{C}H_2$ oligomer), 69.0 (CH oligomer), 71.0 ($CH_2$–$\underline{C}H_2$–O), 71.04 (CH), 73.0 ppm (CH–$\underline{C}H_2$–O).

**Synthesis of MAF–Cl.** 2-Trifluoromethylacryloyl chloride (MAF-Cl) was synthesized by the reaction of 2-trifluoromethylacrylic acid (MAF) (29.1 g, 208 mmol) with phthaloyl dichloride (63.2 g, 311.3 mmol) at 150 °C for 2 h and then 190 °C for 30 min. The product was collected by distillation (Boiling point: 82 °C) during reaction. Yield: 72%, 23.8 g.

Open Access Article. Published on 26 Waysu 2022. Downloaded on 26/08/2024 11:52:58 AM. This article is licensed under a Creative Commons Attribution-NonCommercial 3.0 Unported Licence.

**Synthesis of Pripol–(MAF)$_2$.** Pripol-(MAF)$_2$ monomer was synthesized by adding $NEt_3$ (8.85 g, 87.5 mmol) dropwise to dichloromethane solution of Pripol (15.81 g, 29.2 mmol) and MAF-Cl (11.10 g, 70 mmol) at 0 °C, followed by stirring at room temperature for 4 h. The reaction mixture was washed with 0.5 N hydrochloric acid, saturated aqueous sodium hydrogencarbonate and brine, dried over $MgSO_4$, filtered and dried under reduced pressure to afford the pure di-(trifluoro)methacrylate (Pripol-(MAF)$_2$) as a yellow liquid. Yield: 80%, 18.3 g.

$^1$H-NMR (400 MHz, $CDCl_3$): $\delta$/ppm = 0.89 ppm (m, $CH_3$), 1.02–1.62 ppm (m, $CH_2$–C$\underline{H}_2$–$CH_2$), 1.70 ppm (m, C$\underline{H}_2$–$CH_2$–O), 2.53 ppm (m, CH–C$\underline{H}_2$–$CH_2$), 4.25 ppm (t, C$\underline{H}_2$–O), 6.42 ppm (d, C$\underline{H}$–C), 6.72 ppm (d, C$\underline{H}$–C).

$^{13}$C-NMR (101 MHz, $CDCl_3$): $\delta$/ppm = 14.08 ppm ($\underline{C}H_3$), 22.7 ppm, 25.97 ppm, 28.4–32.02 ppm ($CH_2$–$\underline{C}H_2$–$CH_2$), 28.4 ppm ($\underline{C}H_2$–$CH_2$–O), 31.98 ppm (CH–$\underline{C}H_2$–$CH_2$), 65.96 ppm (t, $\underline{C}H_2$–O), 117.30–125.45 (q, $\underline{C}F_3$), 131.75 ppm (C), 132.46 (q, $\underline{C}H_2$–C), 161.50 ppm (C=O).

$^{19}$F-NMR (377 MHz, $CDCl_3$): $\delta$/ppm = - 65.6 ($CF_3$).

**Synthesis of Pripol-acrylate (Pripol-A$_2$).** Pripol-A$_2$ monomer was synthesized by adding acryloyl chloride (9.05 g, 100.0 mmol, 2.4 equiv.) dropwise to a dichloromethane solution of Pripol (22.58 g, 41.67 mmol, 1 equiv.) and $NEt_3$ (12.65 g, 125 mmol) at 0 °C, followed by stirring at room temperature for 4 h. The reaction mixture was washed with 0.5 N hydrochloric acid, saturated aqueous sodium hydrogencarbonate and brine, dried over $MgSO_4$, filtered and dried under reduced pressure to afford the pure di-acrylate (Pripol-A$_2$) as an orange liquid. Yield: 85%, 23 g.

$^1$H-NMR (400 MHz, $CDCl_3$): $\delta$/ppm = 0.89 ppm (m, $CH_2$–C$\underline{H}_3$), 1.02–1.62 ppm (m, $CH_2$–C$\underline{H}_2$–$CH_2$), 1.69 ppm (m, C$\underline{H}_2$–$CH_2$–O), 2.56 ppm (m, CH–C$\underline{H}_2$–$CH_2$), 4.17 ppm (t, C$\underline{H}_2$–O), 5.84 ppm (d, C$\underline{H}$–C, $^2J$ = 1.5 Hz, $^3J$ = 10.4 Hz), 6.14 ppm (d, C$\underline{H}$–C–C=O, $^3J$ = 17.3 Hz, 10.4 Hz), 6.42 ppm (m, C$\underline{H}$–C, $^2J$ = 1.5 Hz, $^3J$ = 17.3 Hz).

$^{13}$C-NMR (101 MHz, $CDCl_3$): $\delta$/ppm = 14.04 ppm ($\underline{C}H_3$), 22.90 ppm, 26.10 ppm, 28.5–31.80 ppm ($CH_2$–$\underline{C}H_2$–$CH_2$), 29.0 ppm ($\underline{C}H_2$–$CH_2$–O), 32.00 ppm (CH–$\underline{C}H_2$–$CH_2$), 64.70 ppm ($\underline{C}H_2$–O), 128.60 ($\underline{C}$H–C–C=O), 130.50 ($\underline{C}H_2$–C), 166.24 ppm (C=O).

**$^{19}$F-NMR kinetic monitoring.** Typically, BMA-MAF-TBE (0.317 g, 1 equiv.) was mixed with MAF-Me (0.154 g, 1 equiv.) in DMF-d7 at a concentration of 1 M. The mixture was then homogenized by vortex stirring and 450 μL were transferred into an NMR tube. The reaction was then monitored by $^{19}$F-NMR at 60 °C at fixed time intervals using a Bruker Avance III 400 MHz NMR spectrometer. The same procedure was applied with BMA-MAF-Me and MAF-TBE.

**Procedure of CANs synthesis.** The β-aminoester network (BAE) containing fluorine and hydroxyl group (BAE–F–OH) was synthesized from Pripol-(MAF)$_2$ (8.65 g, 2 equiv.) and BD-β-HA (1.61 g, 1 equiv.). BAE–F was obtained from Pripol-(MAF)$_2$ (8.64 g, 2 equiv.) and BA (1.12 g, 1 equiv.) and BAE–OH was obtained from Pripol-A$_2$ (7.15 g, 2 equiv.) and BD-β-HA (1.61 g, 1 equiv.). All the reactive mixture was initially mixed 1 min using a Speed-Mixer. Then BAE–F–OH and BAE–F were left at room temperature overnight, before to be shaped at the hot press for 1 h under 3 *t* at respectively 100 °C and 120 °C. After mixing, BAE–OH was poured into a silicone mold and cured 24 h at 100 °C.

**Reshaping procedure.** The reprocessing behavior of the materials was examined using a Carver 3960 manual heating press. BAE–F–OH, BAE–F and BAE–OH samples were respectively pressed at 100, 120 and 150 °C for 1 h under 3 *t*, and then were cooled to room temperature (*ca.* 25 °C) before removing from the hot press.

## Results & discussion

### Aza-Michael addition

As previously demonstrated with a thia-Michael reaction, the presence of a $CF_3$ group in α position of a Michael acceptor facilitates the addition of Michael donors thanks to the strong electron-withdrawing effect of such a substituent.[43,44] Here, the same effect was observed for the aza-Michael reaction with *N*-benzylmethylamine (BMA) (Scheme 1). Indeed, the reaction with *tert*-butyl 2-(trifluoromethyl)acrylate (MAF-TBE) was performed at room temperature in 10 minutes in DCM whereas the reaction with *tert*-butyl acrylate (A-TBE) required a temperature of 70 °C and 24 h to occur under solvent-free conditions. The model molecules BMA-MAF-TBE and BMA-A-TBE (Fig. S1 and S2†) were both obtained in high yields and characterized by $^1$H-NMR, $^{13}$C-NMR, and additionally by $^{19}$F-NMR for BMA-MAF-TBE.

These model molecules were used to specifically evaluate the aza-Michael exchange reaction. For that purpose, BMA-MAF-TBE and BMA-A-TBE were left to react with methyl 2-trifluoromethylacrylate (MAF-Me) or methylacrylate (A-Me) and the formation of respectively BMA-MAF-Me and BMA-A-Me by exchange of Michael acceptor was monitored over time (Scheme 2). BMA-MAF-Me (Fig. S3†) and BMA-A-Me (Fig. S4†) were also separately synthesized to determine their NMR signatures. These reactions were performed using a 1 : 1 BMA-X-TBE : acrylate ratio in DMF at 60 °C and 1 M of each adduct, and were monitored by $^{19}$F-NMR and $^1$H-NMR. No exchange was observed for the non-fluorinated system even after 48 h of reaction, whereas 18% of BMA-MAF-TBE was already converted to BMA-MAF-Me after only 1 h. These results clearly indicate that the presence of a $CF_3$ group drastically accelerate the exchange reaction. Hence, the inductive effects of the $CF_3$ group play a key role on the aza-Michael exchange rate, they activate both the dissociation of β-amino esters, and the addition of amines onto fluorinated double bonds.

Two additional exchange reactions were examined (Fig. 1): the reaction of BMA-MAF-TBE with MAF-Me and that of BMA-MAF-Me with MAF-TBE. The formation and disappearance of the different MAF adducts were monitored by $^{19}$F-NMR over 24 h. The formations of BMA-MAF-TBE and BMA-MAF-Me were characterized by the appearance of two signals for each compound: a doublet at −67.39 and a triplet at −65.76 ppm for BMA-MAF-TBE and a doublet at −67.32 and a triplet at −65.50 for BMA-MAF-Me respectively. Both experiments led to the same final BMA-MAF-TBE/BMA-MAF-Me mixture with a 60/40 mol% ratio (Fig. 1). Hence it appears that BMA-MAF-Me is relatively less stable than BMA-MAF-TBE. These preliminary results highlighted the potential of fluorine-activated aza-Michael as

Open Access Article. Published on 26 Waysu 2022. Downloaded on 26/08/2024 11:52:58 AM.
This article is licensed under a Creative Commons Attribution-NonCommercial 3.0 Unported Licence.

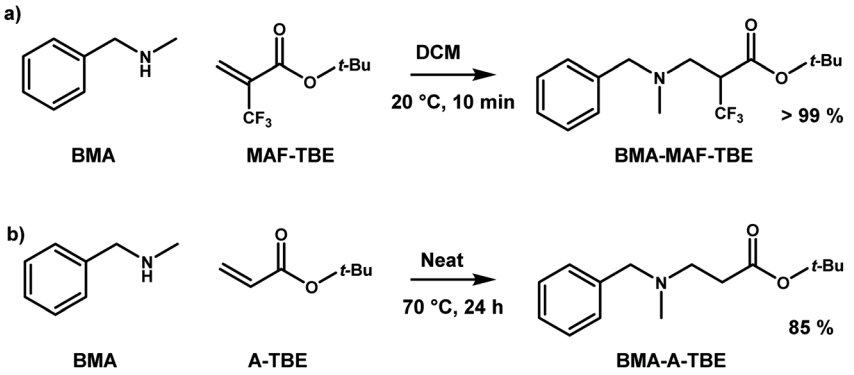


Scheme 1 Aza-Michael addition of N-benzylmethylamine on (a) *tert*-butyl 2-(trifluoromethyl)acrylate (MAF-TBE) and (b) *tert*-butyl acrylate (A-TBE).

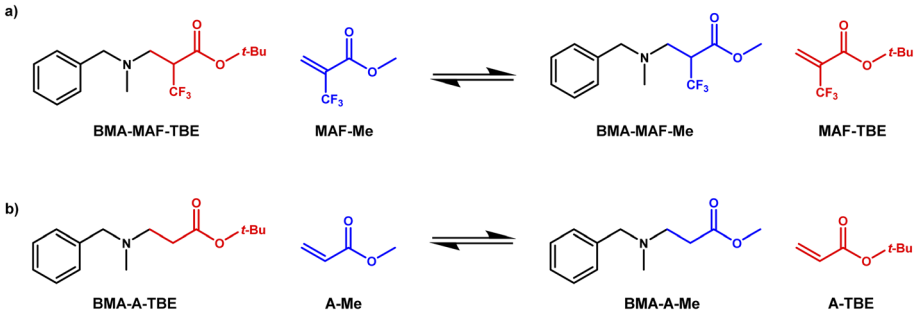


Scheme 2 Aza-Michael exchange reactions.

a fast exchange reaction for CAN application. Note that in the materials, the dissociation of the β-aminoesters would likely be more activated (faster) than that of the model compounds due to higher steric hindrance in this preliminary study compared to the following material study.

## Material synthesis and characterizations

Following these encouraging results on model molecules, the objective was to prepare β-amino ester (BAE) biobased CANs by aza-Michel polyaddition in order to reduce their impact on the environment. Therefore, biobased *bis*-acrylate and *bis*-amine

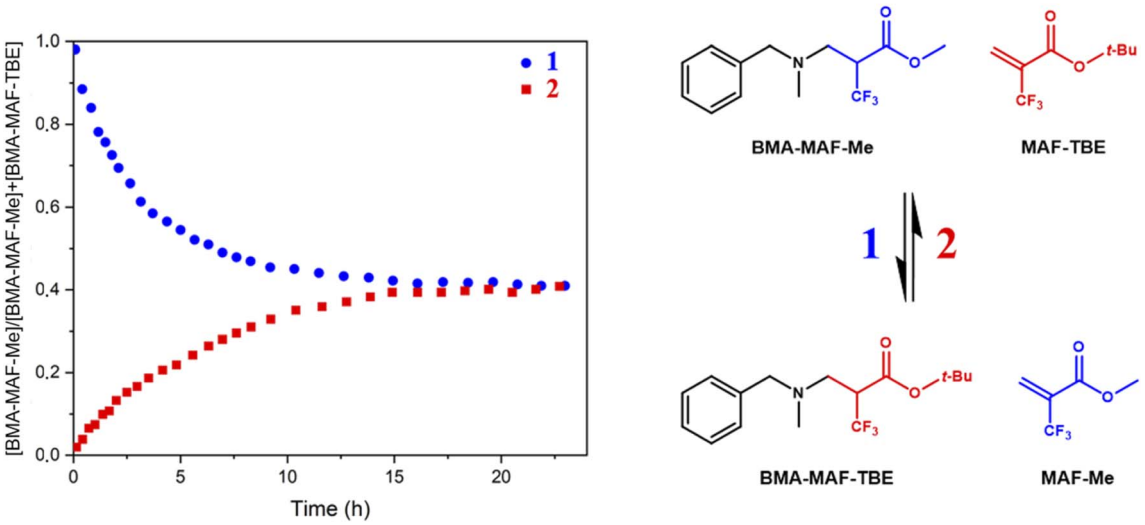


Fig. 1 Kinetic monitoring of BMA-MAF-TBE and BMA-MAF-Me exchange reactions at 1 M by $^{19}$F-NMR in DMF-$d_7$ at 60 °C.

Open Access Article. Published on 26 Waysu 2022. Downloaded on 26/08/2024 11:52:58 AM.
This article is licensed under a Creative Commons Attribution-NonCommercial 3.0 Unported Licence.

monomers needed to be synthesized from natural resources. Since a primary amine can add onto two acrylates successively, a *bis*-amine is a potential tetra-functional monomer allowing the formation of a cross-linked network. Moreover, in addition to the exchangeable aza-Michael adducts presented in the network, ester functions could also undergo exchange in the presence of hydroxy functions, leading to a synergistic effect in CANs. Hence, butanediol-di-β-hydroxyamine (BD-β-HA) was used to introduce hydroxy groups in the network.

BD-β-HA was synthesized from butanediol diglycidyl ether (BDGE), itself prepared from butanediol and epichlorohydrin, both of which can be biobased. Indeed, butanediol can be obtained from carbohydrates produced by hydrolysis of starch or bacteria fermentation, and epichlorohydrin can be synthesized from glycerol.[45,46] Moreover, β-hydroxyamines are known for their facile synthesis, and their high reactivity toward epoxides,[47] cyclic carbonates[48] and Michael acceptors[42] compared to conventional alkylamines due to the H-bonding assistance of the β-OH substituent. BD-β-HA was chosen for three main reasons: its chemical structure enabling the combination of aza-Michael addition and transesterification reaction with its β-OH substituent, its higher reactivity toward Michael acceptors and finally its eco-friendly synthesis. To obtain BD-β-HA, BDGE was reacted with aqueous ammonia in a single step using a sealed reactor and the reaction product was characterized by $^{1}$H-NMR and $^{13}$C-NMR (Fig. S5†). Since the primary amines formed during the synthesis can still react with the starting epoxide, some BD-β-HA oligomers, are formed. The amount of oligomers was determined by $^{1}$H-NMR (signal at 3.88 ppm) to be 16 mol%.

Using a Green Chemistry approach,[49] Pripol™ 2033, a fully biobased diol derived from fatty acids, was used to prepare Pripol *bis*-(trifluoromethyl)acrylate (Pripol-(MAF)$_2$) and Pripol *bis*-acrylate (Pripol-A$_2$) (Fig. 2). 2-Trifluoromethylacryloyl chloride or acryloyl chloride were added to the diols in the presence of NEt$_3$ at low temperature to prepare the two desired bis-esters. The resulting Pripol-(MAF)$_2$ and Pripol-A$_2$ monomers featured a high biobased carbon content, of respectively 82% and 86%. Pripol-(MAF)$_2$ (Fig. S6†) and Pripol-A$_2$ (Fig. S7†) were both characterized by $^{1}$H and $^{13}$C-NMR and by $^{19}$F-NMR for Pripol-(MAF)$_2$.

The activating role of the CF$_3$ group on the aza-Michael exchange that was highlighted at the molecular level could be efficiently implemented in CANs. Three β-amino ester (BAE) thermosets were synthesized *via* aza-Michael addition (Table 1). BAE–F–OH was prepared by reaction of Pripol-(MAF)$_2$ with BD-β-HA. This material thus contained β-amino-α–CF$_3$–ester moieties able to undergo both CF$_3$-activated aza-Michael exchange reactions and transesterification. BAE–F was prepared from 1,4-bis(3-aminopropoxy)butane (BDA) and Pripol-(MAF)$_2$. This material was thus devoid of hydroxy groups for transesterification reactions, but still fairly prone to aza-Michael exchange *via* CF$_3$-activation. Finally, BAE–OH was synthesized from Pripol-A$_2$ and BD-β-HA. This third material thus contained free hydroxy groups able to trigger transesterification, but was devoid of CF$_3$ activating groups. The study of the relaxation behaviours of these three thermosets should allow to determine the influence of each NGP on their CAN properties. Note that thanks to the use of biobased monomers, BAE–F–OH, BAE–OH and BAE–F were composed of 84%, 87% and 74% of biobased carbons respectively.

Because of the difference in reactivity between the four monomers, the curing conditions of each thermoset were different, depending on whether the double bond was activated by a CF$_3$ group or not, in agreement with the model reaction study. In the cases of BAE–F–OH and BAE–F, both containing CF$_3$ activating groups, a strong gel was formed after only 1 min of stirring in a SpeedMixer at 25 °C. Therefore, BAE–F–OH and BAE–F were shaped by compression molding at 100 °C and 120 °C for 1 h respectively. In contrast, BAE–OH was cured in an oven at 80 °C for 24 h in a silicon mold. Indeed, without the CF$_3$-activation of the double bond, the crosslinking was much slower and the mixture remained liquid after mixing at 25 °C, highlighting the gap of reactivity compared to BAE–F–OH and BAE–F. In these two materials, the CF$_3$-activation of the Michael acceptors was so strong that the aza-Michael crosslinking was too fast to permit monitoring by rheometry (the gel point could not be determined). Moreover the effect of the hydroxy groups on the aza-Michael additions could not be observed as BAE–F–OH and BAE–F showed the same ultra-fast curing behavior.

No residual exothermy was observed by DSC (Fig. S8†) for any of the materials indicating that they were fully cured under the

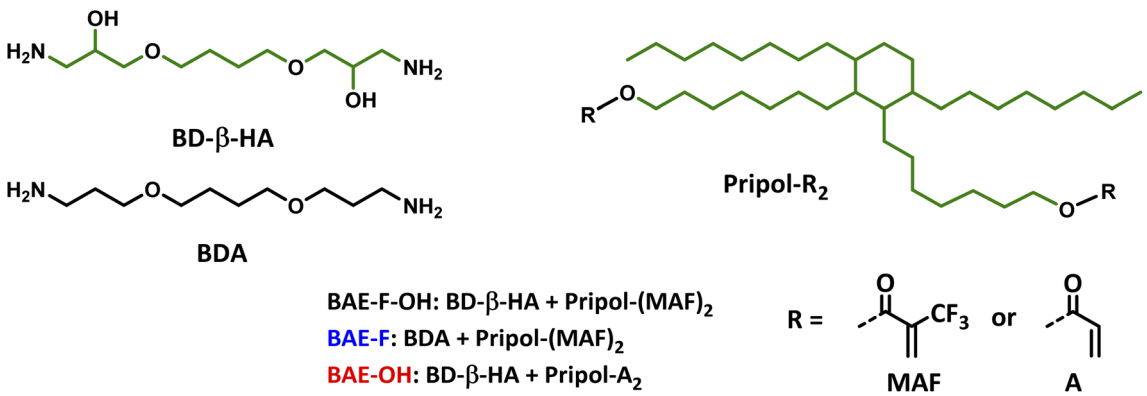


Fig. 2 Monomer structures used for the synthesis of BAE networks, the green carbons correspond to biobased carbon.

Open Access Article. Published on 26 Waysu 2022. Downloaded on 26/08/2024 11:52:58 AM.
This article is licensed under a Creative Commons Attribution-NonCommercial 3.0 Unported Licence.

Table 1 Overview of β-amino esters (BAE) composition and biobased carbon content associated

| | Acrylate | | Amine | | | |
|---|---|---|---|---|---|---|
| CAN | Pripol-(MAF)2 (equiv.) | Pripol-$A_2$ (equiv.) | BD-β-HA (equiv.) | BDA (equiv.) | Curing conditions | Biobased carbon content (mol%) |
| BAE–F–OH | 2 | — | 1 | — | 20 °C 12 h + 1 h 100 °C[a] | 84 |
| BAE–F | 2 | — | — | 1 | 20 °C 12 h + 1 h 120 °C[a] | 74 |
| BAE–OH | — | 2 | 1 | — | 80 °C 24 h | 87 |

[a] Under 3 *t* of compression.

Table 2 Overview of physical properties of β-amino esters (BAE)

| | $T_g$ (°C) | $T_\alpha$ (°C) | $T_{d5\%}$ (°C) | $E'_{glassy}$[a] (GPa) | $E'_{rubbery}$[b] (MPa) | Gel content (%) |
|---|---|---|---|---|---|---|
| BAE–F–OH | −38 | −23 | 252 | 1.8 | 3.4 | 86 ± 2 |
| BAE–F | −22 | −25 | 255 | 1.5 | 2.9 | 91 ± 3 |
| BAE–OH | −38 | −33 | 297 | 1.9 | 2.1 | 83 ± 1 |

[a] Determined at $T_\alpha$ − 50 °C. [b] Determined at $T_\alpha$ + 50 °C.

preparation conditions used. Interestingly, the glass transition temperatures of BAE–F–OH and BAE–OH were identical (−38 °C) suggesting that the $CF_3$ groups had no impact on the chain movement in these materials (Table 2). The $T_g$ of BAE–F was expected to be lower than those of the other materials because of the additional hydrogen bonds provided by the hydroxy functions. However, the presence of BD-β-HA oligomers tends to decrease the $T_g$ by decreasing the AHEW, while commercial BDA is only composed of primary amines. In BAE–F–OH or BAE–OH longer polymer chains are present compared to BAE–F, hence providing more flexibility to these networks and thus explaining the $T_g$ values measured. The gel contents of the BAE networks were comparable (>83%) and confirmed the formation of highly cross-linked networks.

The three BAE networks were also analyzed by DMA as shown in Fig. 3. The storage moduli on the glassy and rubbery plateau of the three materials were of the same order of magnitude. According to the results of the thermogravimetric analyses (Fig. S9†), the thermal stabilities of the fluorinated BAEs (BAE–F and BAE–F–OH) were identical, indicating that the hydroxy group did not significantly affect the material degradation. BAE–OH showed a higher $T_{d5\%}$, possibly because the aza Michael exchange reactions were slower in this material. This phenomenon was already noticed by Du Prez *et al.*[41] who demonstrated that aza-Michael dissociation could be related to thermal degradation. Indeed, as the aza-Michael exchange is assumed to follow a dissociative mechanism, network degradation is dependent on the exchange rate of this reaction and therefore on the temperature.

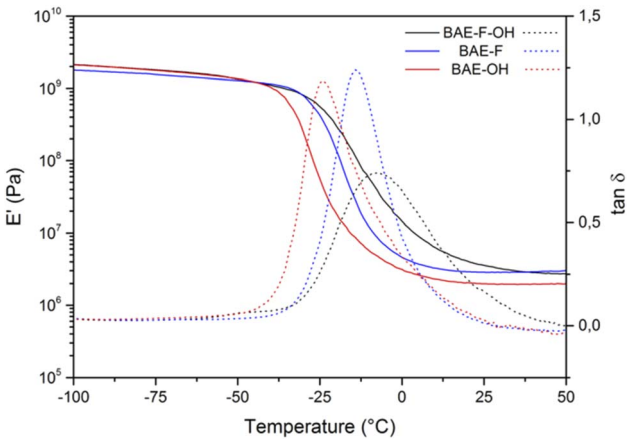


Fig. 3 Storage modulus (full curves) and tan(δ) (dotted curves) for BAE–F–OH (black curve), BAE–F (blue curve) and BAE–OH (red curve).

## Dynamic properties

In order to study the dynamic character of the three BAE networks, they were subjected to stress-relaxation experiments (Fig. 4 (normalized data) and Fig. S10† (non-normalized data)). A 1% shear strain was applied and the relaxation modulus (G(t)) was monitored as a function of time. As mentioned previously, BAE–F, which can only relax stress *via* fluorine-activated aza-Michael exchange due to the absence of hydroxyl groups, clearly demonstrated faster relaxation than previously reported CANs based on non-fluorinated aza-Michael exchange. Indeed, even if the comparison is not totally exact because of polymer matrix difference, relaxation times were up to 20 times lower at 130 °C for BAE–F compared to these non-fluorinated CANs.[41,42] This result is in good agreement with the preliminary molecular study that highlighted the strong activation of aza-Michael exchange induced by fluorine atoms.

Recently, CANs having two coexisting mechanisms have gained a lot of interest.[50] Some CANs have been based on this concept, for instance disulfide metathesis was combined with transesterification in epoxy vitrimer.[51] Du Prez *et al.* also studied

Open Access Article. Published on 26 Waysu 2022. Downloaded on 26/08/2024 11:52:58 AM.
This article is licensed under a Creative Commons Attribution-NonCommercial 3.0 Unported Licence.

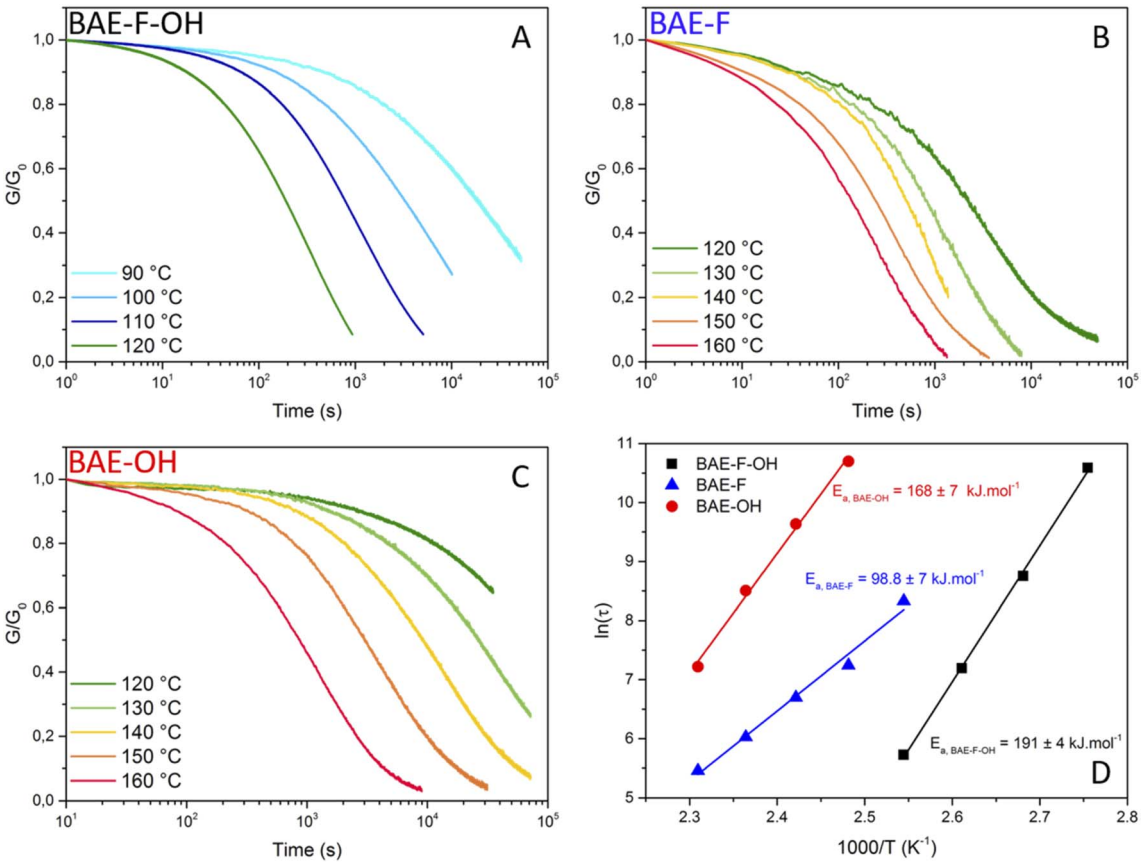


Fig. 4 Normalized stress-relaxation curves at different temperatures for a 1% strain (A) for BAE–F–OH, (B) for BAE–F and (C) for BAE–O. (D) Fitting of the relaxation time ($\tau$) *vs.* temperature data by the Arrhenius equation for BAE–F–OH (black squares), BAE–F (blue triangle) and BAE–OH (red circles).

dynamic thiol–yne cross-linking as a new platform for the exchange of thioacetal linkages and demonstrated that associative and dissociative mechanisms occurred concomitantly.[52] Following the development of these dual systems previously reported,[51,53,54] BAE–F–OH was synthesized to produce a network in which aza-Michael exchange and transesterification can concomitantly occur. Both exchange reactions were activated by the presence of the $CF_3$ group in the alpha and beta positions of the ester function and of the nitrogen atom respectively. Moreover, the polymerization by aza-Michael addition results in the presence of tertiary amines in the network which were previously proven to promote transesterification.[37] The comparison of the stress relaxation experiments at 120 °C (Fig. 5A) highlights the interest of using a dual CANs network. Indeed, the fastest relaxation was displayed by BAE–F–OH, in which, both $CF_3$-activated aza-Michael and transesterification reactions can occur, compared to BAE–F for which only fluorine-activated aza-Michael exchange is at play. Finally, the activation effect of the $CF_3$ group was particularly underlined by the comparison of BAE–F–OH and BAE–OH. Indeed, in the absence of $CF_3$ groups in $\alpha$-position of the ester functions (BAE–OH), the network relaxation was drastically slowed down.

Each material was studied in a specific temperature range as their relaxation rate were very different: stress-relaxations were performed from 90 to 120 °C for BAE–F–OH (Fig. 4A), from 120 to 160 °C for BAE–F (Fig. 4B) and from 120 to 160 °C for BAE–OH (Fig. 4C). Even if the aza-Michael exchange reaction apparently proceeds *via* a dissociative mechanism, Arrhenius behaviors were observed for all the BAE networks, and specifically for BAE–F which is based only on aza-Michael exchange. These observations confirm that dissociative CANs can follow an Arrhenius law in a specific range of temperature as recently highlighted by Dichtel and Elling.[22] $E_{a,flow}$ of 191 ± 4 kJ mol$^{-1}$, 98.8 ± 7 kJ mol$^{-1}$ and 168 ± 7 kJ mol$^{-1}$ were determined for BAE–F-OH, BAE–F and BAE–OH respectively (Fig. 4D). Even if comparing these $E_{a,flow}$ values when multiple exchange reactions are at play is complex, the high activation energy displayed by BAE–F–OH is very promising for future industrial applications. Indeed, ideal CANs should not creep at their service temperature, but be able to reshape in a matter of seconds and at moderate temperature to avoid degradation. Therefore the synthesis of CANs endowed with high activation energy and short relaxation times is desirable as these kind of CANs would demonstrate high viscosity-temperature dependence and high creep resistance.

Open Access Article. Published on 26 Waysu 2022. Downloaded on 26/08/2024 11:52:58 AM.
This article is licensed under a Creative Commons Attribution-NonCommercial 3.0 Unported Licence.

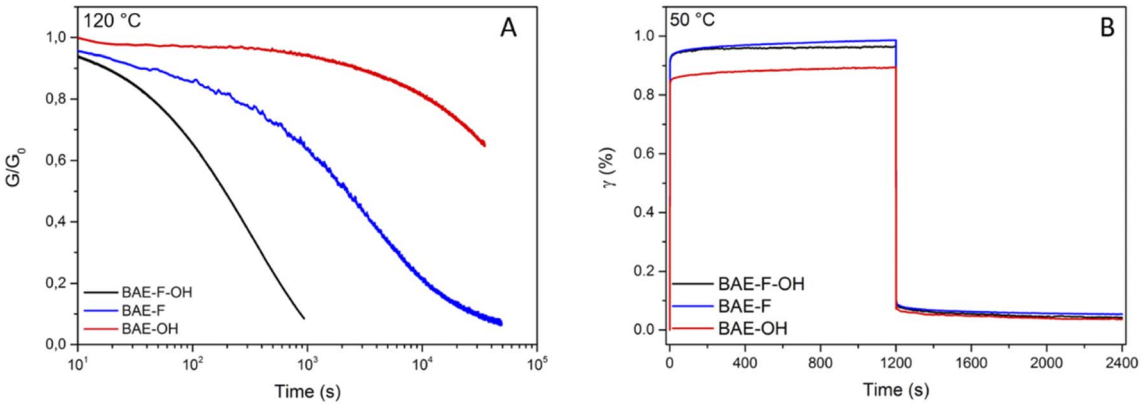


Fig. 5 (A) Normalized stress relaxation of BAEs at 120 °C for a 1% strain (B) creep and recovery data for BAEs at 50 °C for an applied stress of 2 kPa.

Additionally, creep experiments were performed at 50 °C (Fig. 5B) and 80 °C (Fig. S11†) on the three BAE CANs to further demonstrate the sensitivity of the materials to temperature. After the creep-recovery experiments at 80 °C, BAE–F–OH and BAE–F showed permanent deformations of 0.16% and 0.07% respectively, whereas the deformation of BAE–OH was only of 0.03% (Fig. S11†). Hence, at 80 °C, exchange reactions occurred in BAE–F-OH and BAE–F whereas no exchange reaction took place in BAE–OH, highlighting once again the activating effect of $CF_3$ groups. However, at 50 °C, the three BAEs showed the same small permanent deformation (<0.03%). BAE–F–OH and BAE–F were as creep resistant as BAE–OH at low temperature indicating slow exchange reactions in all three materials. However, these exchange reactions were easily set off at moderate temperature thanks to the $CF_3$-activation, while higher temperatures, favoring degradations, were necessary to trigger these reactions in BAE–OH. These different results are in agreement with previous reports, where high activation flow energy was related to materials with strong creep resistance.[29,41,55]

In conclusion, the presence of fluorinated groups in these CANs clearly accelerated the aza-Michael exchange reaction and the transesterification. Moreover, a synergistic effect is at play when both aza-Michael and transesterification are complementary used. Finally, biobased CANs with high activation energies were obtained *via* the combination of $CF_3$-activated (and amine catalyzed) transesterification and aza-Michael exchanges, affording higher creep resistance at low temperature (50 °C) and faster reshaping at moderate to high temperature (100 °C to 150 °C).

## Reshaping

In order to demonstrate the reprocessability of the BAE networks, samples were cut into small pieces (approximately 2/2 mm square) and reshaped under different conditions using a hot press (Fig. 6). All samples were subjected to a 1 h treatment under 3 *t* of pressure, but the reshaping temperature was chosen accordingly to the relaxation analyses performed in the previous section. The reprocessing temperatures were 100 °C, 120 °C and 150 °C for BAE–F–OH, BAE–F and BAE–OH respectively. The three materials were reshaped three times and characterized after each reprocessing (Table S1†).

The TGA thermograms of the cured and reshaped samples were almost perfectly superimposable and featured an identical mass loss profile (Fig. S9†), suggesting that the materials were not structurally degraded during the reshaping process. The TGA thermograms also indicated that the thermal degradation temperature of the materials was superior to the reshaping temperature. The chemical integrity of the three networks after reprocessing was confirmed by ATR-FTIR spectroscopy (Fig. S11†). The potential formation of amides resulting from the dissociation of aza-Michael adduct followed by the attack of this amine on an ester was not observed by FTIR. Moreover, the reshaping did not significantly impact the $T_g$ or the $T_\alpha$ of the BAEs networks confirming the conservation of the network structure after reshaping. The swelling index (SI) and gel content (GC) of the materials were also evaluated after each reprocessing cycle. No critical difference was observed for BAE–F–OH and BAE–F whereas the SI and GC of BAE–OH respectively increased and decreased with the number of reshaping cycles. This suggest that the degree of crosslinking decreased slightly in BAE–OH after each reshaping cycle. Finally, DMA analyses (Fig. S12†) showed that the moduli of BAE–F–OH and BAE–F were not significantly impacted by the reprocessing as observed in other CANs materials.[56,57] Their values on the glassy and the rubbery plateau remained almost constant. This demonstrates that even though these CANs are partially based on dissociative reaction, there were no loss of crosslinking density upon reshaping. In contrast the moduli of BAE–OH decreased after each reshaping confirming the loss of crosslinking suggested by the evolution of the gel content and swelling index of this material. Although the reasons for this behaviour are not perfectly clear, it may be caused by thermal degradation due to a prolonged treatment at relatively high temperature compared to the others material. The difference of mechanism involved between each materials could potentially also explained this specific behaviour for BAE–OH.

Open Access Article. Published on 26 Waysu 2022. Downloaded on 26/08/2024 11:52:58 AM.
This article is licensed under a Creative Commons Attribution-NonCommercial 3.0 Unported Licence.

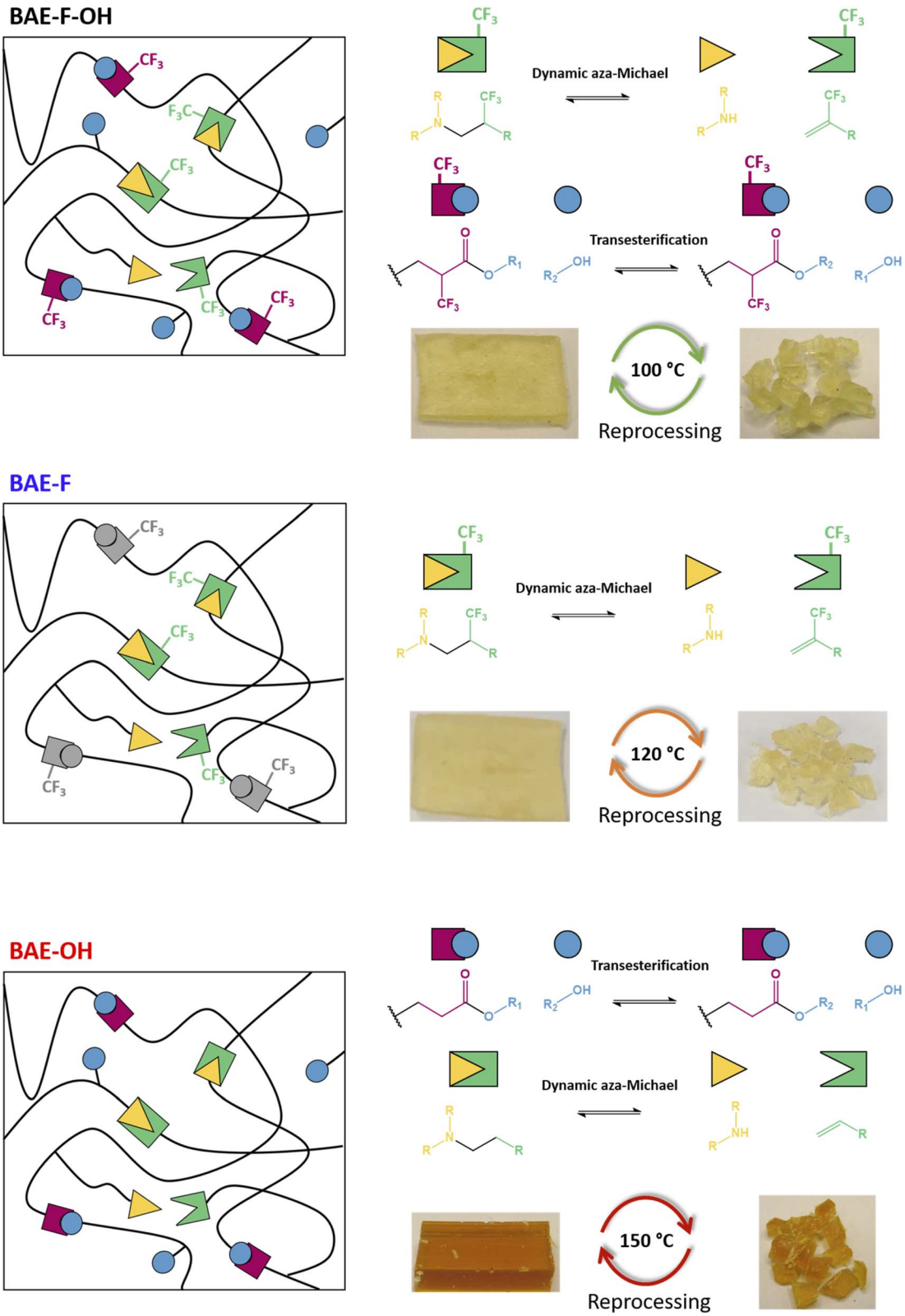


Fig. 6 Schematic representations of BAE–F–OH, BAE–F and BAE–OH associated with their respective exchange reactions and reprocessing conditions.

Open Access Article. Published on 26 Waysu 2022. Downloaded on 26/08/2024 11:52:58 AM.
This article is licensed under a Creative Commons Attribution-NonCommercial 3.0 Unported Licence.

## Conclusion

The influence of a $CF_3$ group on the aza-Michael addition and on the reversibility of the reaction was first highlighted on model molecules. Whereas no exchange was observed between aza-Michael adduct and acrylate at 60 °C, the introduction of a $CF_3$ group on the acrylate double bond led to a high exchange rate (18% of exchange in 1 h) under the same conditions.

Based on this preliminary molecular study, new biobased monomers derived from Pripol™ 2033 and butanediol diglycidyl ether were synthesized and used to prepare CANs containing up to 87 mol% of renewable carbons. Three CANs based on aza-Michael and/or transesterification exchange reactions were synthesized. The high reactivity of the 2-trifluoromethylacrylate moiety toward aza-Michael addition afforded easy access to catalyst-free networks at room temperature. Moreover, the synergistic effect of the aza-exchange/transesterification and the accelerating effect related to the presence of trifluoromethyl groups were separately evaluated by studying respectively non-hydroxylated and non-fluorinated materials. Indeed, hydroxyl-containing fluorinated material took only 102 s to relax 35% of the initial modulus at 120 °C whereas 912 s and 28 842 s were necessary for the fluorinated only and hydroxyl-containing only materials respectively.

The synergistic combination of the two exchange reactions afforded CANs (BAE–F–OH and BAE–OH) with high activation energy reducing their creep at low temperature compared to the mono-exchange reaction material (BAE–F). The presence of fluorinated group on the α-carbon of the ester and on the β-position of the tertiary amine considerably reduced the necessary reshaping temperature from 150 °C to 100 °C, facilitating material reprocessing, without affecting the creep resistance of the material at lower temperature.

An additive-free CAN based on two different exchange reactions, both accelerated by the same activating group, was thus successfully designed and prepared, and showed remarkable reprocessing abilities. This study contributes to enrich the range of application of fluorinated groups as accelerating substituents for CANs, including overlooked reactions such as the aza-Michael exchange, and illustrates the possibility to prepare a catalyst-free CAN from biobased monomers. Such a strategy should open new opportunities to develop more sustainable materials.

## Conflicts of interest

The authors declare no competing financial interest.

## Acknowledgements

This work was funded by the French National Research Agency ANR (AFCAN project ANR-19-CE06-0014).

## References

1 J. P. Pascault and R. J. J. Williams, *Epoxy Polymers: New Materials and Innovations*, 2010, DOI: 10.1002/9783527628704.
2 D. Montarnal, M. Capelot, F. Tournilhac and L. Leibler, Silica-Like Malleable Materials from Permanent Organic Networks, *Science*, 2011, **334**(6058), 965–968, DOI: 10.1126/science.1212648.
3 J. L. Self, N. D. Dolinski, M. S. Zayas, J. Read De Alaniz and C. M. Bates, Brønsted-Acid-Catalyzed Exchange in Polyester Dynamic Covalent Networks, *ACS Macro Lett.*, 2018, 817–821, DOI: 10.1021/acsmacrolett.8b00370.
4 T. F. Scott, A. D. Schneider, W. D. Cook and C. N. Bowman, Photoinduced Plasticity in Cross-Linked Polymers, *Science*, 2005, **308**(5728), 1615–1617, DOI: 10.1126/science.1110505.
5 N. Zheng, Y. Xu, Q. Zhao and T. Xie, Dynamic Covalent Polymer Networks: A Molecular Platform for Designing Functions beyond Chemical Recycling and Self-Healing, *Chem. Rev.*, 2021, **121**(3), 1716–1745, DOI: 10.1021/acs.chemrev.0c00938.
6 Y. Yang, Y. Xu, Y. Ji and Y. Wei, Functional Epoxy Vitrimers and Composites, *Prog. Mater. Sci.*, 2021, **120**, 100710, DOI: 10.1016/J.PMATSCI.2020.100710.
7 J. Zheng, Z. M. Png, S. H. Ng, G. X. Tham, E. Ye, S. S. Goh, X. J. Loh and Z. Li, Vitrimers: Current Research Trends and Their Emerging Applications, *Mater. Today*, 2021, **51**, 586–625, DOI: 10.1016/J.MATTOD.2021.07.003.
8 N. J. Van Zee and R. V. Nicolaÿ, Permanently Crosslinked Polymers with Dynamic Network Topology, *Prog. Polym. Sci.*, 2020, **104**, 101233, DOI: 10.1016/J.PROGPOLYMSCI.2020.101233.
9 J. M. Winne, L. Leibler and F. E. Du Prez, Dynamic Covalent Chemistry in Polymer Networks: A Mechanistic Perspective, *Polym. Chem.*, 2019, **10**(45), 6091–6108, DOI: 10.1039/C9PY01260E.
10 F. I. Altuna, U. Casado, I. E. Dell'Erba, L. Luna, C. E. Hoppe and R. J. J. Williams, Epoxy Vitrimers Incorporating Physical Crosslinks Produced by Self-Association of Alkyl Chains-SI, *Polym. Chem.*, 2020, 1337–1347, DOI: 10.1039/c9py01787a.
11 F. I. Altuna, C. E. Hoppe and R. J. J. Williams, Shape Memory Epoxy Vitrimers Based on DGEBA Crosslinked with Dicarboxylic Acids and Their Blends with Citric Acid, *RSC Adv.*, 2016, **6**(91), 88647–88655, DOI: 10.1039/c6ra18010h.
12 M. Hayashi, R. Yano and A. Takasu, Synthesis of Amorphous Low: T g Polyesters with Multiple COOH Side Groups and Their Utilization for Elastomeric Vitrimers Based on Post-Polymerization Cross-Linking, *Polym. Chem.*, 2019, **10**(16), 2047–2056, DOI: 10.1039/c9py00293f.
13 W. Denissen, G. Rivero, R. Nicolaÿ, L. Leibler, J. M. Winne and F. E. Du Prez, Vinylogous Urethane Vitrimers, *Adv. Funct. Mater.*, 2015, **25**(16), 2451–2457, DOI: 10.1002/adfm.201404553.
14 Y. Spiesschaert, C. Taplan, L. Stricker, M. Guerre, J. M. Winne and F. E. Du Prez, Influence of the Polymer Matrix on the Viscoelastic Behaviour of Vitrimers, *Polym. Chem.*, 2020, **11**(33), 5377–5385, DOI: 10.1039/d0py00114g.
15 A. Chao, I. Negulescu and D. Zhang, Dynamic Covalent Polymer Networks Based on Degenerative Imine Bond Exchange: Tuning the Malleability and Self-Healing Properties by Solvent, *Macromolecules*, 2016, **49**(17), 6277–

Open Access Article. Published on 26 Waysu 2022. Downloaded on 26/08/2024 11:52:58 AM.
This article is licensed under a Creative Commons Attribution-NonCommercial 3.0 Unported Licence.

6284, DOI: 10.1021/ACS.MACROMOL.6B01443/ASSET/IMAGES/LARGE/MA-2016-01443X_0008.JPEG.

16 G. Zhang, Q. Zhao, L. Yang, W. Zou, X. Xi and T. Xie, Exploring Dynamic Equilibrium of Diels–Alder Reaction for Solid State Plasticity in Remoldable Shape Memory Polymer Network, *ACS Macro Lett.*, 2016, **5**(7), 805–808, DOI: 10.1021/acsmacrolett.6b00357.

17 X. Kuang, G. Liu, X. Dong and D. Wang, Correlation between Stress Relaxation Dynamics and Thermochemistry for Covalent Adaptive Networks Polymers, *Mater. Chem. Front.*, 2016, **1**(1), 111–118, DOI: 10.1039/C6QM00094K.

18 D. Pratchayanan, J.-C. Yang, C. L. Lewis, N. Thoppey and M. Anthamatten, Thermomechanical Insight into the Reconfiguration of Diels–Alder Networks, *J. Rheol.*, 2017, **61**(6), 1359–1367, DOI: 10.1122/1.4997580.

19 L. Zhang and S. J. Rowan, Effect of Sterics and Degree of Cross-Linking on the Mechanical Properties of Dynamic Poly(Alkylurea–Urethane) Networks, *Macromolecules*, 2017, **50**(13), 5051–5060, DOI: 10.1021/acs.macromol.7b01016.

20 M. Hayashi and L. Chen, Functionalization of Triblock Copolymer Elastomers by Cross-Linking the End Blocks *via* Trans-N -Alkylation-Based Exchangeable Bonds, *Polym. Chem.*, 2020, **11**(10), 1713–1719, DOI: 10.1039/C9PY01759C.

21 P. Chakma, C. N. Morley, J. L. Sparks and D. Konkolewicz, Exploring How Vitrimer-like Properties Can Be Achieved from Dissociative Exchange in Anilinium Salts, *Macromolecules*, 2020, **53**(4), 1233–1244, DOI: 10.1021/acs.macromol.0c00120.

22 B. R. Elling and W. R. Dichtel, Reprocessable Cross-Linked Polymer Networks: Are Associative Exchange Mechanisms Desirable?, *ACS Cent. Sci.*, 2020, **6**(9), 1488–1496, DOI: 10.1021/acscentsci.0c00567.

23 M. Capelot, D. Montarnal, F. Tournilhac and L. Leibler, Metal-Catalyzed Transesterification for Healing and Assembling of Thermosets, *J. Am. Chem. Soc.*, 2012, **134**(18), 7664–7667, DOI: 10.1021/ja302894k.

24 M. Capelot, M. M. Unterlass, F. Tournilhac and L. Leibler, Catalytic Control of the Vitrimer Glass Transition, *ACS Macro Lett.*, 2012, **1**(7), 789–792, DOI: 10.1021/mz300239f.

25 K. Yu, P. Taynton, W. Zhang, M. L. Dunn and H. J. Qi, Reprocessing and Recycling of Thermosetting Polymers Based on Bond Exchange Reactions, *RSC Adv.*, 2014, **4**(20), 10108–10117, DOI: 10.1039/c3ra47438k.

26 J. P. Brutman, P. A. Delgado and M. A. P. HillmyerVitrimers, *ACS Macro Lett.*, 2014, **3**(7), 607–610, DOI: 10.1021/mz500269w.

27 Z. Yang, Q. Wang and T. Wang, Dual-Triggered and Thermally Reconfigurable Shape Memory Graphene-Vitrimer Composites, *ACS Appl. Mater. Interfaces*, 2016, **8**, 37, DOI: 10.1021/acsami.6b07403.

28 T. Liu, B. Zhao and J. Zhang, Recent Development of Repairable, Malleable and Recyclable Thermosetting Polymers through Dynamic Transesterification, *Polymer*, 2020, **194**, 122392, DOI: 10.1016/j.polymer.2020.122392.

29 M. Guerre, C. Taplan, J. M. Winne and F. E. Du Prez, Vitrimers: Directing Chemical Reactivity to Control Material Properties, *Chem. Sci.*, 2020, **11**(19), 4855–4870, DOI: 10.1039/D0SC01069C.

30 F. Cuminet, S. Caillol, É. Dantras, É. Leclerc and V. Ladmiral, Neighboring Group Participation and Internal Catalysis Effects on Exchangeable Covalent Bonds: Application to the Thriving Field of Vitrimer Chemistry, *Macromolecules*, 2021, **54**(9), 3927–3961, DOI: 10.1021/acs.macromol.0c02706.

31 J. Han, T. Liu, C. Hao, S. Zhang, B. Guo and J. Zhang, A Catalyst-Free Epoxy Vitrimer System Based on Multifunctional Hyperbranched Polymer, *Macromolecules*, 2018, **51**(17), 6789–6799, DOI: 10.1021/acs.macromol.8b01424.

32 T. Liu, S. Zhang, C. Hao, C. Verdi, W. Liu, H. Liu and J. Zhang, Glycerol Induced Catalyst-Free Curing of Epoxy and Vitrimer Preparation, *Macromol. Rapid Commun.*, 2019, **40**(7), 1800889, DOI: 10.1002/marc.201800889.

33 F. I. Altuna, V. Pettarin and R. J. J. Williams, Self-Healable Polymer Networks Based on the Cross-Linking of Epoxidised Soybean Oil by an Aqueous Citric Acid Solution, *Green Chem.*, 2013, **15**(12), 3360–3366, DOI: 10.1039/c3gc41384e.

34 M. Delahaye, J. M. Winne and F. E. Du Prez, Internal Catalysis in Covalent Adaptable Networks: Phthalate Monoester Transesterification As a Versatile Dynamic Cross-Linking Chemistry, *J. Am. Chem. Soc.*, 2019, 15277–15287, DOI: 10.1021/jacs.9b07269.

35 M. Delahaye, F. Tanini, J. O. Holloway, J. M. Winne and F. E. Du Prez, Double Neighbouring Group Participation for Ultrafast Exchange in Phthalate Monoester Networks, *Polym. Chem.*, 2020, **11**(32), 5207–5215, DOI: 10.1039/d0py00681e.

36 Y. Nishimura, J. Chung, H. Muradyan and Z. Guan, Silyl Ether as a Robust and Thermally Stable Dynamic Covalent Motif for Malleable Polymer Design, *J. Am. Chem. Soc.*, 2017, **139**(42), 14881–14884, DOI: 10.1021/jacs.7b08826.

37 F. I. Altuna, C. E. Hoppe and R. J. J. Williams, Epoxy Vitrimers with a Covalently Bonded Tertiary Amine as Catalyst of the Transesterification Reaction, *Eur. Polym. J.*, 2019, **113**, 297–304, DOI: 10.1016/j.eurpolymj.2019.01.045.

38 D. Berne, F. Cuminet, S. Lemouzy, C. Joly-Duhamel, R. Poli, S. Caillol, E. Leclerc and V. Ladmiral, Catalyst-Free Epoxy Vitrimers Based on Transesterification Internally Activated by an α–CF 3 Group, *Macromolecules*, 2022, **55**(5), 1669–1679, DOI: 10.1021/acs.macromol.1c02538.

39 F. Cuminet, D. Berne, S. Lemouzy, E. Dantras, C. Joly-Duhamel, S. Caillol, E. Leclerc and V. Ladmiral, Catalyst-Free Transesterification Vitrimers: Activation *via* α -Difluoroesters, *Polym. Chem.*, 2022, **8**, 5255–5446, DOI: 10.1039/D2PY00124A.

40 S. Lemouzy, F. Cuminet, D. Berne, S. Caillol, V. Ladmiral, R. Poli and E. Leclerc, Understanding the Reshaping of Fluorinated Polyester Vitrimers by Kinetic and DFT Studies of the Transesterification Reaction, *Chem. – Eur. J.*, 2022, **28**(48), e202201135.

41 C. Taplan, M. Guerre and F. E. Du Prez, Covalent Adaptable Networks Using β-Amino Esters as Thermally Reversible

Open Access Article. Published on 26 Waysu 2022. Downloaded on 26/08/2024 11:52:58 AM.
This article is licensed under a Creative Commons Attribution-NonCommercial 3.0 Unported Licence.

Building Blocks, *J. Am. Chem. Soc.*, 2021, **143**(24), 9140–9150, DOI: 10.1021/jacs.1c03316.

42 D. Berne, G. Coste, R. Morales, M. Boursier, J. Pinaud, V. Ladmiral and S. Caillol, Taking Advantage of β-Hydroxy Amine Enhanced Reactivity and Functionality for the Synthesis of Dual Covalent Adaptable Networks, *Polym. Chem.*, 2022, **8**, 5255–5446, DOI: 10.1039/D2PY00274D.

43 T. P. Vasil'eva, A. F. Kolomiets, E. I. Mysov and A. V. Fokin, Comparison of α- and β-Trifluoromethylsubstituted Acrylic Acids in Their Reactions with Thiols, *Russ. Chem. Bull.*, 1997, **46**(6), 1181–1183, DOI: 10.1007/BF02496227.

44 B. Chen, J. Lei and J. Zhao, Michael Addition of Aryl Thiols to 3-(2,2,2-Trifluoroethylidene)Oxindoles under Catalyst-Free Conditions: The Rapid Synthesis of Sulfur-Containing Oxindole Derivatives, *J. Chem. Res.*, 2018, **42**(4), 210–214, DOI: 10.3184/174751918X15240724383170.

45 A. Forte, A. Zucaro, R. Basosi and A. Fierro, LCA of 1,4-Butanediol Produced *via* Direct Fermentation of Sugars from Wheat Straw Feedstock within a Territorial Biorefinery, *Materials*, 2016, **9**(7), 1–22, DOI: 10.3390/MA9070563.

46 A. Canela-Xandri, M. Balcells, G. Villorbina, P. Christou and R. Canela-Garayoa, Preparation and Uses of Chlorinated Glycerol Derivatives, *Molecules*, 2020, **25**(11), 2511.

47 A.-S. Mora, R. Tayouo, B. Boutevin, G. David and S. Caillol, Vanillin-Derived Amines for Bio-Based Thermosets, *Green Chem.*, 2018, **20**(17), 4075–4084, DOI: 10.1039/C8GC02006J.

48 B. Quienne, R. Poli, J. Pinaud and S. Caillol, Enhanced Aminolysis of Cyclic Carbonates by β-Hydroxylamines for the Production of Fully Biobased Polyhydroxyurethanes, *Green Chem.*, 2021, **23**(4), 1678–1690, DOI: 10.1039/D0GC04120C.

49 J. Liu, S. Wang, Y. Peng, J. Zhu, W. Zhao and X. Liu, Advances in Sustainable Thermosetting Resins: From Renewable Feedstock to High Performance and Recyclability, *Prog. Polym. Sci.*, 2021, **113**, 101353, DOI: 10.1016/J.PROGPOLYMSCI.2020.101353.

50 M. Podgórski, N. Spurgin, S. Mavila and C. N. Bowman, Mixed Mechanisms of Bond Exchange in Covalent Adaptable Networks: Monitoring the Contribution of Reversible Exchange and Reversible Addition in Thiol–Succinic Anhydride Dynamic Networks, *Polym. Chem.*, 2020, **11**(33), 5365–5376, DOI: 10.1039/d0py00091d.

51 M. Chen, L. Zhou, Y. Wu, X. Zhao and Y. Zhang, Rapid Stress Relaxation and Moderate Temperature of Malleability Enabled by the Synergy of Disulfide Metathesis and Carboxylate Transesterification in Epoxy Vitrimers, *ACS Macro Lett.*, 2019, **8**(3), 255–260, DOI: 10.1021/acsmacrolett.9b00015.

52 N. Van Herck, D. Maes, K. Unal, M. Guerre, J. M. Winne and F. E. Du Prez, Covalent Adaptable Networks with Tunable Exchange Rates Based on Reversible Thiol–Yne Cross-Linking, *Angew. Chem., Int. Ed.*, 2020, **59**(9), 3609–3617, DOI: 10.1002/anie.201912902.

53 J. O. Holloway, C. Taplan and F. E. Du. Prez, Combining Vinylogous Urethane and β-Amino Ester Chemistry for Dynamic Material Design, *Polym. Chem.*, 2022, **13**(14), 2008–2018.

54 Z. Liu, Y. Ma, Z. Zhang, Z. Shi and J. Gao, Rapid Stress Relaxation, Multistimuli-Responsive Elastomer Based on Dual-Dynamic Covalent Bonds and Aniline Trimer, *Langmuir*, 2022, **38**(16), 4812–4819, DOI: 10.1021/ACS.LANGMUIR.1C03241.

55 L. Li, X. Chen, K. Jin, M. B. Rusayyis and J. M. Torkelson, Arresting Elevated-Temperature Creep and Achieving Full Cross-Link Density Recovery in Reprocessable Polymer Networks and Network Composites *via* Nitroxide-Mediated Dynamic Chemistry, *Macromolecules*, 2021, **54**(3), 1452–1464, DOI: 10.1021/acs.macromol.0c01691.

56 J. J. Lessard, L. F. Garcia, C. P. Easterling, M. B. Sims, K. C. Bentz, S. Arencibia, D. A. Savin and B. S. Sumerlin, Catalyst-Free Vitrimers from Vinyl Polymers, *Macromolecules*, 2019, **52**(5), 2105–2111, DOI: 10.1021/acs.macromol.8b02477.

57 S. Debnath, S. Kaushal and U. Ojha, Catalyst-Free Partially Bio-Based Polyester Vitrimers, *ACS Appl. Polym. Mater.*, 2020, **2**(2), 1006–1013, DOI: 10.1021/acsapm.0c00016.